

Article

From TLS to VLS: Biomass Estimation at Individual Tree Level

Yi Lin *, Anttoni Jaakkola, Juha Hyypä and Harri Kaartinen

Finnish Geodetic Institute, Department of Remote Sensing and Photogrammetry, P.O. Box 15, 02431 Masala, Finland; E-Mails: anttoni.jaakkola@fgi.fi (A.J.); juha.hyypa@fgi.fi (J.H.); harri.kaartinen@fgi.fi (H.K.)

* Author to whom correspondence should be addressed; E-Mail: yi.lin@fgi.fi; Tel.: +358-9-295-55-240; Fax: +358-9-295-55-200.

Received: 30 May 2010; in revised form: 18 June 2010 / Accepted: 7 July 2010 /

Published: 26 July 2010

Abstract: This study explores the applicability of vehicle-based laser scanning (VLS) for biomass estimation at individual tree level, since biomass serves as an essential biophysical parameter indicating tree health. Previous work suggests that terrestrial laser scanning (TLS) has been primarily validated for biomass prediction, however, in subject to laborious relocation in practice. VLS, as an advanced mode of TLS with more flexible mobility and also high sampling density, can work as a new efficient technique for surveying single trees. Combined with the positive binds between the biomass and TLS-samplings during manual defoliation, this work aims to seek the relations between biomass and VLS-samplings, by correlating the VLS- and TLS-samplings within the same crowns during natural foliation. The resulting R^2 values of the two correlations after normalization are larger than 0.88 and 0.61, respectively, and the associated root mean square errors (RMSEs) are less than 0.051 and 0.076. VLS, thus, can be validated for estimating biomass at the individual tree level, with the TLS-investigated data as a bridging reference.

Keywords: biomass estimation; VLS; TLS; serial retrieval model

1. Introduction

Biomass serves as an important biophysical parameter appropriate for assessing a diversity of natural characteristics, from tree health, forest regeneration, biological balance, to energy conversion [1]. The biomass-associated studies are helpful for reflecting various processes of biophysicochemical variations,

e.g., the situation of tree growth, the decrease of local carbon dioxide, the expansion of plant diseases, and the damage of forest fires. The relevant topics e.g., “Why is the spatial distribution of biomass important in understanding the carbon cycle?” and “How well do we know the biomass of the world’s forests?” have been discussed in [2,3], and these researches, however, must be undertaken after the biomass in the objected region is measured. Therefore, this study focuses on the concrete methods for acquiring biomass values. Biomass in ecology is defined to be the amount of living matter in a given habitat, and is commonly expressed as the weight of organisms per unit area. Obviously, weighting is not available for many situations. Hence, a great amount of approaches for obtaining biomass indirectly have been proposed, as reviewed as follows.

The biomass quantification or estimation methods have been developed long before from ground-based destructive weighting [2], space-borne optical remote sensing (RS) [4] to synthetic aperture radar (SAR) [5], which are involved with different contexts, e.g., spatial resolutions or earth surfaces. The destructive weighting method is conducted by removing the leaves and branches from trees step by step, and then weighting the cut-off materials successively. This direct measurement means is accurate but laborious and expensive. Moreover, destructive weighting biomass is forbidden in most environments. Satellite-based optical RS as a kind of indirect method has been applied extensively to retrieve biomass [6]. The correspondences between biomass and pixel values have been tested with convincing results, and the utilized parameters include e.g., reflectance [7], greenness [8], canopy density [9], brightness temperature [10], and, sometimes, their combinations. RS images are applicable for estimating biomass at large region-wise scales, while the optical sensors are apt to suffer from saturation in spectral response to the dense canopies with high biomass [11]. The radar-based methods are less weather-dependent and capable of producing data from large areas with high temporal resolutions [12], but for single tree level the related accuracies generally are not satisfactory.

As the state-of-the-art technology, airborne laser scanning (ALS), often termed as light detection and ranging (LiDAR), has been adopted as an attractive measure for biomass detection, due to its capability to directly measure canopy structures and stand attributes [13,14]. Biomass can be derived from these attributes, and the relevant variables include e.g., tree height, diameter at breast height (DBH), and wood density. There are several recent studies in which methods have been developed towards more accurate ALS-based biomass detection [15-17]. LiDAR has also been tried to integrate with other kinds of techniques [18,19]. Most results, however, suggest that LiDAR tends to underestimate tree heights due to large probabilities of missing treetops even with high sampling densities [20,21]. The relatively low density of current ALS systems cannot reflect canopy structure comprehensively. Therefore, ALS has been utilized mostly for stand- or regional-wise estimations of tree characteristics [22-24]. ALS-based biomass estimation at individual tree level was also validated [25] not long before.

Terrestrial laser scanning (TLS) occurs as an effective and low-cost means for biomass investigation of individual trees, as its fine spatial resolution and small beam size allow the inner parts of crowns to be measured with detailed information [26]. This makes it possible to estimate biomass accurately, and the performances of TLS apparatuses have been steadily increasing [27]. With these favorable factors, the appearances of TLS in tree inventory tasks have also been increasing, and the relevant applications include measuring e.g., canopy structure [28], leaf area index (LAI) [29], foliage-height profile [30] and

timber volume [31]. These works can help biomass estimation indirectly, and direct biomass estimation has also been conducted with a primarily verified result [32]. However, in terms of efficiency, TLS suffers from the laborious relocations when surveying multi-plots of trees.

Recently, vehicle-based laser scanning (VLS) as a newly-developed surveying, mapping, and RS technology has attracted a lot of attention, and the typical VLS systems include e.g., the StreetMapper system [33], the ROAMER system [34], and the Lynx system [35]. The VLS-related surveying module can be installed on various platforms, e.g., minivans, railway carts, and boats as listed in the summary review in [36] for different applications. The associated methods for data processing and information extraction concerning VLS point clouds can be referred to [37-43]. Technically, the common side-view mapping mechanism of VLS is similar with the conventional TLS systems, and simultaneously, VLS has the more flexible mobility than TLS. Therefore, biomass estimation based on VLS seems to be theoretically feasible, while the relevant studies have been few carried out.

From literature review, it can be learnt that the previous works on biomass estimation have mostly been undertaken at stand- and region-scales. Biomass estimation at individual tree level has just begun, while the progress encounters the time-consuming issue during moving TLS. Thus, the objective of this study is to explore the applicability of VLS for biomass estimation. The primary procedures are planned as follows: first, the correlations between the accurately measured biomass and TLS-samplings in laboratory are calculated for different tree species as the standard references; second, the relations between VLS- and TLS-samplings of the same trees are sought; third, the biomass value of each tree surveyed by VLS is achieved based on the serial retrieval model. This study highlights on the first and second procedures to establish a new promising methodology of VLS-based biomass estimation. The consistency of foliage changes influencing laser pulse returns, during manual defoliation in laboratory and natural foliation when VLS monitoring, is also involved.

The organization of the paper is as follows. After background introduction and literature review, Section 2 presents the materials necessary for validating VLS for biomass estimation. Section 3 then describes the proposed methodology for estimating biomass from VLS samplings, which utilizes the associated TLS samplings as references. In Section 4, the experimental results are shown and assessed. Discussions and conclusion are finally presented in Section 5.

2. Data Collection

2.1. Sensei VLS System and Leica HDS6000 TLS System

The VLS systems with high-performance on penetrating crowns are ideal for this study, and Sensei (see Figure 1a) is such a modular surveying system developed at the Finish Geodetic Institute (FGI). Sensei comprises a GPS/IMU positioning system, two laser scanners, a CCD camera, a spectrometer, and a thermal camera. In this study, only the geo-referenced point clouds sampled by LUX are referred. The distance measurement range of Sensei is from 0.3 to 200 m (50 m-targets with 10% remission), and the ranging accuracy is 10 cm. Besides, the divergences of laser beams are 0.08° horizontally and 0.8° vertically with the scanner axes as the references. These parameters are appropriate for measuring the basic data to validate the feasibility of VLS-based biomass estimation.

The Ibeo Lux laser scanner can receive echoes from four different vertical profiles simultaneously, and is also theoretically able to measure up to 38000 points/second if only one return per pulse per profile is recorded. Actually, the scanner can record up to three returns per pulse, which allows Sensei to receive the reflected hits from the backsides of trees or vegetations. This is the advantage of the Sensei VLS system applied for biomass investigation. The point clouds, collected with Ibeo Lux by recording all the four profiles per scan line and all the three echoes per laser pulse, were used as the experimental data.

Figure 1. (a) The Sensei VLS system. (b) The Leica HDS6000 TLS system.



The synchronous reference data was investigated by the Leica HDS6000 TLS system (Figure 1b). HDS6000 is a kind of 685 nm phase-based continuous wave laser scanner with a $360^\circ \times 310^\circ$ field-of-view upwards. This scanner uses a silicon avalanche photo diode (APD) as the photo detector. The distance measurement accuracy is 4–5 mm, and the angular resolution is selectable from 0.009° to 0.288° . The circular beam diameter at the exit and the beam divergence are 3 mm and 0.22 mrad, respectively. These parameters can help the system measure the fine architectures of canopies. After geo-referencing, the associated point clouds within crowns can be segmented as a link between VLS samplings and the destructive-weighting data in laboratory.

2.2. TLS-Biomass Data Acquired in Laboratory

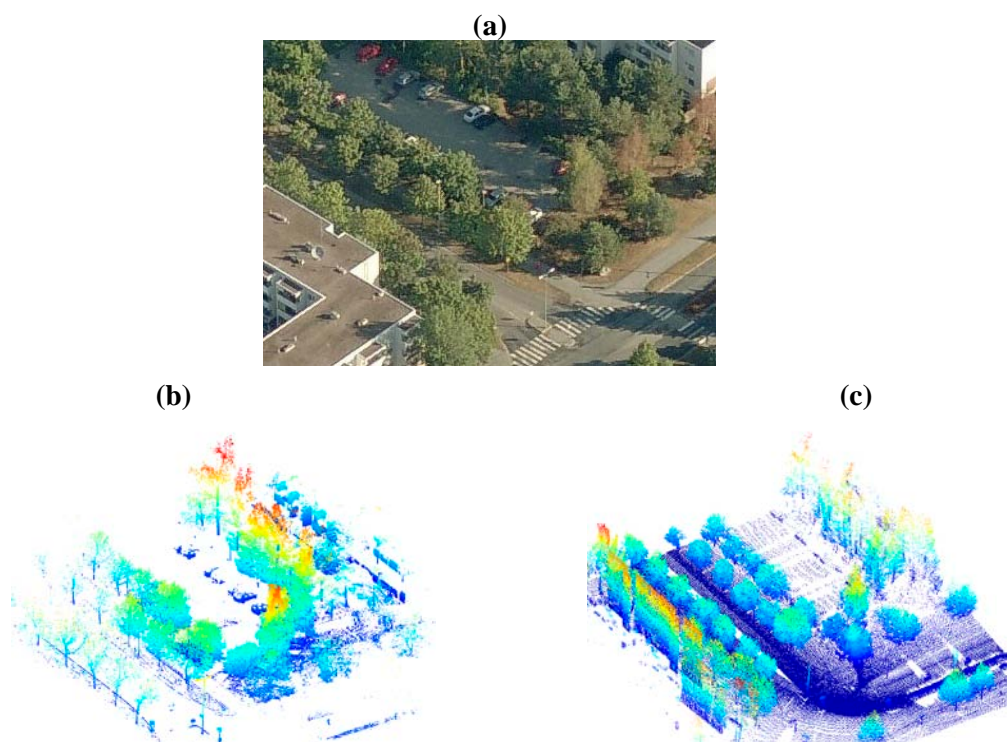
The so-called TLS-biomass data denotes the synchronous measurements of the same trees by TLS and destructive weighting. The experiments were carried out in FGI laboratory. The coniferous species of five pines (Scots Pine) and five spruces (Norway Spruce, *Picea abies*) were first measured with HDS6000 from aside on 20 July 2009, and the deciduous species of 10 birches (Finland Birch) were measured in the same way based on the FARO Photon120 laser scanner, which had almost the same sampling setups with respect to HDS6000, on 28 May 2010. The crowns were firstly scanned by TLS producing the point cloud with number of T_1 , and then the leaves and branches of all the crowns were removed from outside step by step. The cut-off materials were weighted and recorded, and meanwhile, the remaining trees were scanned by TLS. These two procedures were iterated three times per tree, resulting in the biomass samples of b_1 , b_2 , and b_3 and the numbers T_2 , T_3 , and T_4 of TLS-samplings.

At last, the left trunks were measured as b_4 , and 40 pairs of TLS-biomass data $\left\{ \left(b_{ij}, T_{ij} \right)_{i=1, \dots, 5, j=1, \dots, 10} \right\}$ were generated. The subscript i denotes the operation times, and j indicates the sequential number of each tree. Actually, b_{ij} and T_{ij} have no direct relations, instead of $b_{ij} \sim T_{ij} - T_{i(j+1)}$ or $T_{ij} \sim \sum_{k=i}^4 b_{kj}$. Therefore, the relationship between the TLS-biomass data can be sought in terms of the differentiation of TLS-samplings *versus* biomass or the integration of the weighted biomass *versus* TLS-samplings. As the experiments were carried out with critical procedures, the results can offer the fundamental references to inversely retrieve the distribution of biomass from the in-field TLS-sampling.

2.3. VLS-TLS Data Collected in the Study Site

The similar-termed VLS-TLS data was collected in the Espoonlahti test site of Finland on 6 May, 14 May, 28 May, 8 June, and 2 July 2009 separately, which correspond to different foliage phases appropriate for validating the study goal. The six study areas lie around a block, which were scanned by VLS and TLS synchronously. The airborne RS image of one area is illustrated (Figure 2a), and the point clouds collected by TLS and VLS are also demonstrated (Figure 2b,c). From the figures, it can be noticed that many trees were surveyed by both VLS and TLS, notwithstanding probably from different views. There are also buildings and poles mixed in the scenes, and they can be interpreted out from TLS and VLS point clouds. The study site can be used as the typical area to validate the new technique, and 12 trees (containing deciduous and coniferous trees) producing 60 pairs of VLS-TLS samples were extracted for numerical analysis.

Figure 2. (a) The airborne RS image of the first study area. (b) The associated point cloud investigated by TLS. (c) The related point cloud collected by VLS. Different colors denote different heights, and red indicates the largest altitudes in (b) and (c).



3. Methods

3.1. Geo-referencing

After the surveying work was finished, geo-referencing was the first step of data post-processing, since the initial data had only the ranging information. Geo-referencing can give the corresponding 3D coordinates to the recorded echo points, and the approaches of converting the unorganized points into regular spatial distributions must be tackled accurately, as the overlaps of crowns caused by coarse positioning of points may introduce large errors during point number statistics. Sensei utilizes direct geo-referencing, where GPS/IMU measurements are applied to derive the position and attitude of the system platform and each instrument. This information is then employed to calculate the 3D positions of all the received laser points.

Direct geo-referencing is noted mathematically by a transformation between the local coordinates specified in the sensor (TLS or camera) frame and the geodetic (mapping) reference frame with Equation (1)

$$\vec{X}^e = \vec{X}_{IMU}^e + R_b^e R_s^b \left[\lambda \vec{x}^s + \Delta \vec{X}_{IMU}^s \right] \quad (1)$$

where \vec{X}^e are the object coordinates in the earth-centered and earth-fixed (ECEF) frame, \vec{X}_{IMU}^e denote the IMU coordinates in ECEF frame, R_b^e signifies the rotation matrix from body frame to ECEF frame, R_s^b denotes the rotation matrix from sensor frame to body frame, \vec{x}^s are the object coordinates in sensor frame, $\Delta \vec{X}_{IMU}^s$ delegate the level arm between IMU and sensor. The value of IMU coordinates \vec{X}_{IMU}^e and rotation matrix R_b^e can be calculated from IMU outputs, R_s^b is sought in field calibration, and lever arm $\Delta \vec{X}_{IMU}^s$ are obtained using a tape measure.

3.2. Crown Segmentation

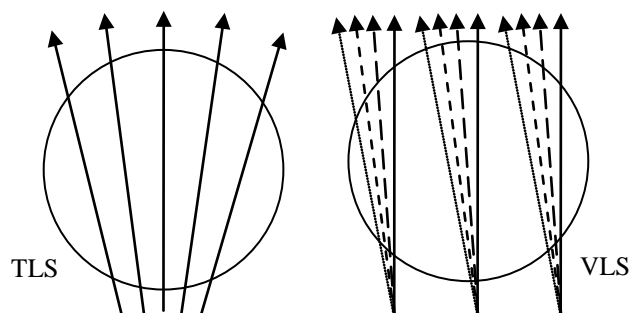
Since this study focuses on the statistical properties of the sampling points within crowns, critical registration is not a necessary step in pre-processing. Alternatively, segmenting the objected crowns precisely is more important. The second step, thus, is to segment the single crowns by Terrascan [44], which is a commercial software solution for processing laser scanning points for numerical analysis. Terrascan can efficiently handle millions of points, as all the routines have been tweaked for optimum performance. The operations of crown segmentation for VLS- and TLS-collected point clouds are the same in Terrascan. The objective trees can be located according to the pre-set references, and the fence can be drawn around the point collections corresponding to a single crown. Then, all the points, with their projections in the fence, can be segmented and stored into an isolated file. Processing on details can be conducted aiming at some special points, and the unnecessary or erroneous points can be deleted.

3.3. Scanning Model Analysis

The accumulative numbers of points within the crowns segmented from VLS- and TLS-measured point clouds individually cannot be utilized directly for comparison, as the associated sampling modes

are different. The scanning models of the applied VLS and TLS systems need to be analyzed, and the correspondence is better to be acquired and uniformed firstly. In terms of the scan line schematics, respectively demonstrated in Figure 3, the arrangements of scan lines and the angles between the laser pulses in profiles are dissimilar, and uniformization of samplings is the premier for seeking the binds between VLS and TLS samplings. Scanning model analysis mainly refers to two steps, namely number uniformization of the scan lines in each crown space and angle uniformization between the pulses in each profile.

Figure 3. Schematic models of TLS and VLS scanning examined from top view. TLS has scan lines in radial form, and VLS comprises multi-profiles in the parallel scan lines.



TLS works in a rotating mode, and the scan lines distribute in a star-radiating form. The scan lines occupy a consistent angle from the top view, and the number of scan lines lying in the more distant crowns will become less. The pulses in the same profiles are also in a star-radiating mode from up to down, and thus, the point number along distance attenuates as deduced in Equation (2)

$$N_{nT} = N_{mT} (d_n/d_{mT})^2 \quad (2)$$

where N_{mT} is the number of points sampled within each crown, d_{mT} denotes the distance from TLS to the crown center, d_n is the prescribed distance for the uniformized comparisons between TLS and VLS samplings, and N_{nT} is the number after uniformization. HDS6000 is a phase-based scanner, and the phenomenon of multi-echoes related to one laser pulse can be neglected.

VLS works under the pattern of sideways-scanning, and its scan lines distribute in a parallel-arranged form. From the perspective of scan line, the number of points lying in the more distant crowns will still remain equal. The Ibeo LUX laser scanner can emit four laser beams simultaneously for each scan line, and there is a 0.8° angle between them. Each two corresponding profiles in the parallel scan lines can also be deemed to be parallel. The pulses in the same profiles, however, are in a star-radiating mode, and the point number in each profile follows the linear attenuation rule with respect to distance, as shown in Equation (3)

$$N_{nV} = N_{mV} (d_n/d_{mV}) \quad (3)$$

where the variables have the similar meanings as in Equation (2), and the subscripts are replaced to stand for VLS. Ibeo LUX can distinguish as many as three echoes per pulse, and this can produce the effect of penetration.

Besides the hardware-induced differences between the two laser scanners, the concrete surveying modes also introduce some discrepancies that are necessary to consider. The predominant factors include two aspects: the number of scan lines hitting the crowns and the sampling density. Besides the factor of distance from the scanner to the goal crowns mentioned above, another cause for number variation of scan lines, mainly for VLS, is the interval between scan lines, as the mapping vehicle cannot ensure a constant velocity. The intervals between the scan lines in some crowns are unavoidably larger than the other ones. At the same time, the sampling frequency of VLS is often different from the stable TLS systems, and a coefficient as the adjusting parameter according to the prescribed setups is added in. The uniformization of interval and density mainly involved with VLS samplings can be expressed in Equation (4)

$$N_{nV} = c(s_n/s_{mV})(d_n/d_{mV})N_{mV} \quad (4)$$

where s_{mV} is the real interval between the scan lines, and s_n is the uniformized interval, which is defined according to the mean number of scan lines of TLS in the same crown. c is the coefficient for density uniformization.

3.4. Serial Retrieval Model

The correlation work of TLS-biomass data is fulfilled in two ways, namely between the normalized total biomass of each crown and the normalized total hits from the same crown, and the normalized branch and leaf biomass of each crown *versus* the normalized hits from the same crown. As the stems grow slowly and will show no clear variation in the second surveying lasting for three months, only the later situation is considered in this study. The same operations are undertaken in the following VLS-TLS data correlation. Then, the serial retrieval model based on VLS-samplings, TLS-samplings and the biomass data is built to form a complete frame for biomass prediction.

The implementations are to achieve the relations between TLS-samplings and biomass as references, and then seek the correspondence between VLS- and TLS-samplings to validate VLS-based biomass estimation. If there is a positive correlation existing (best in linear form), VLS can be verified capable of mapping biomass of trees in practical applications. The correspondence is quantified by computing Pearson correlation coefficients, which can reflect the consistency degree between the two different sampling modes and biomass weights. Regression analysis, next, is employed on the two sets of data to seek the fitting functions individually.

If two linear functions are obtained with promising results, e.g., with lower root mean square error (RMSE), the serial retrieval model revealing the relationships between VLS-samplings and biomass through TLS-samplings can be established. With the serial linear retrieval model, the status of model fitting and the statistical significances of the estimated parameters can be assessed. The goodness of fitting is commonly checked by calculating the coefficient of determination, e.g., R-square. Analysis of the pattern of residuals and hypothesis testing can also be implemented. Statistical significance can be checked by an F-test of the overall fit, followed by t-tests of individual parameters.

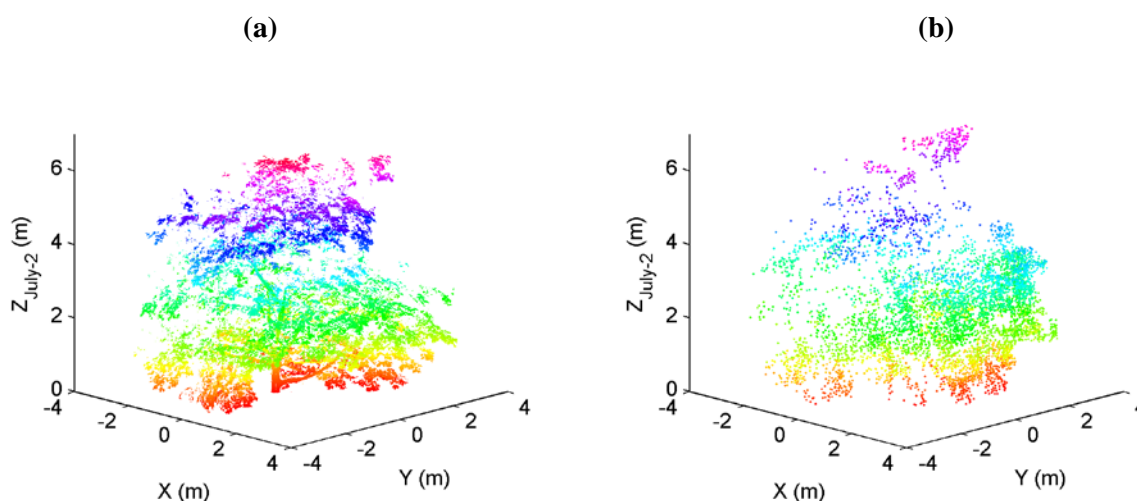
4. Results

The correlations of 40 pairs of deciduous TLS-biomass data, 40 pairs of coniferous TLS-biomass data, and 60 pairs of VLS-TLS data were deployed separately, and the results seem to be satisfactory. The temporary outputs of each recursive step will not be listed in this paper, and the outcomes of the three key procedures, which correspond to crown segmentation, TLS-biomass correlation and VLS-TLS correlation, are described as follows.

4.1. Crown Segmentation

After geo-referencing, 12 typical isolated trees with good appearances both in VLS and TLS point clouds were picked up and segmented out. As the monitoring processes mainly focus on the progress of foliation, the relevant crowns were further extracted as targets. The segmenting operation was based on Terrascan, which can also output the total number of points within each crown efficiently. One pair of crowns of the same tree reconstructed from VLS and TLS data is illustrated in Figure 4. Both VLS data and TLS data can reflect the structure of the tree well, and this also shows the effect of geo-referencing to some extent. It can be recognized that the TLS-measured points are denser than the VLS-scanned ones, and the positioning accuracy is also better than VLS. But this has no much influence to this study, as the statistical total number is concerned for biomass estimation.

Figure 4. Illustrations of the crowns reconstructed by the (a) TLS-; and (b) VLS-collected samplings. Different colors denote different heights.

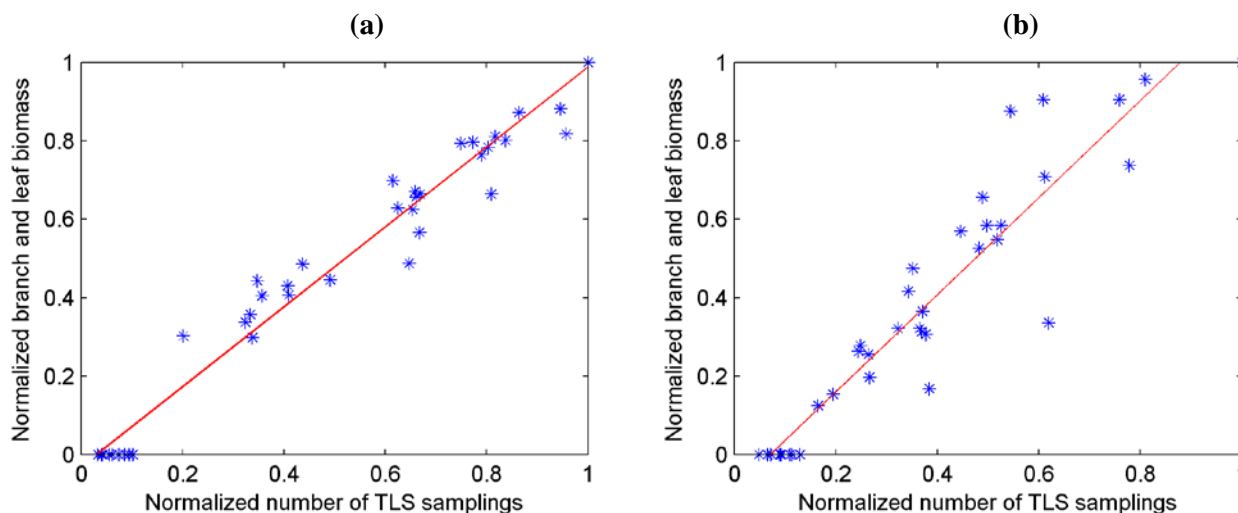


4.2. TLS-Biomass Correlation

As to the laboratory experiments, the relative number of hits from each tree by TLS was used as a predictor of biomass. The maximum number of points within crowns was normalized into 1, when no manual defoliation occurred. The correlation results of the TLS-biomass data are shown in Figure 5, in which the deciduous and coniferous tree species are processed separately. The R^2 based on a linear regression model were 0.97 for the coniferous trees and 0.88 for the deciduous trees respectively. The coefficients of the fitting linear function are listed in Table 1, and the errors can be indicated by RMSE.

Based on parameter comparison, the foliation process of the deciduous trees has more influences to the correlations than the coniferous trees, since the broad leaves are more irregular than the needle leaves. The resulting good relationships both, still, can suggest the feasibility of TLS for biomass estimation.

Figure 5. Correlations of the normalized TLS-biomass data for different tree species after laboratory experiments. **(a)** For the coniferous tree species, $R^2 = 0.97$. **(b)** For the deciduous tree species, $R^2 = 0.88$. The plot-points lying on the horizontal axis at the bottom-left corner correspond to the destructive weightings of the remaining stems.



4.3. VLS-TLS Correlation

In VLS-TLS correlation, 60 pairs of samples relevant to five surveying days were matched statistically. The distribution trend of the point numbers of the VLS-samplings and the TLS-samplings was derived. The hit-numbers were normalized after the samples with the maximum numbers were sought, both in VLS and TLS data. The statistical result is manifested in Figure 6. As the differences of VLS and TLS sampling mechanisms are more complex than the nominated factors listed in sub-Section 3.3 (e.g., multi-conditioned mobility with acceleration), the coefficient of determination is less than the results of TLS-biomass data measured in laboratory. The value of linear slope after fitting is 0.86, and the intercept is 0.07. The coefficient of determination is 0.61, which suggests that VLS-samplings and TLS-samplings still can represent the same crowns in consistency.

Based on the results (Table 1) from subsections 4.2 and 4.3, the serial linear retrieval model can be constructed. The RMSEs of the three regressions are all less than 0.1, and the slopes of the three fittings are close to 1. The serial linear retrieval model for the Espoonlahti test site can be simplified as $Biomass_{Normalized} = 1.07 * VLS_{Normalized} - 0.0024$, which is tackled based on the deciduous TLS-biomass data. The biomass of the little trees measured in laboratory are only at the scales of several kilograms, while the real trees surveyed in the study sites even weigh several tons. Thus, the coefficients of the fitting lines for the biomass and VLS-samplings in practical applications will be somehow different, and the parameters sought in this study cannot be applied directly for other surveying tasks. For real applications, the concrete parameters shall be recalculated as follows: Some typical little trees in the objected region are fell down and implemented destructive weighting and TLS scanning firstly, and

VLS-TLS data is secondly measured in the same region. The data post-processing then can employ the same procedures of this study, and the more accurate parameters can be achieved.

Figure 6. The normalized numbers of VLS samplings *versus* of TLS samplings in the Espoonlahti site; $R^2 = 0.61$. The clustering phenomenon at the bottom-left corner is yielded by two coniferous trees, which have no large biomass changes during foliage flourishing. The points far from the fitted line are caused by crown-shading partially.

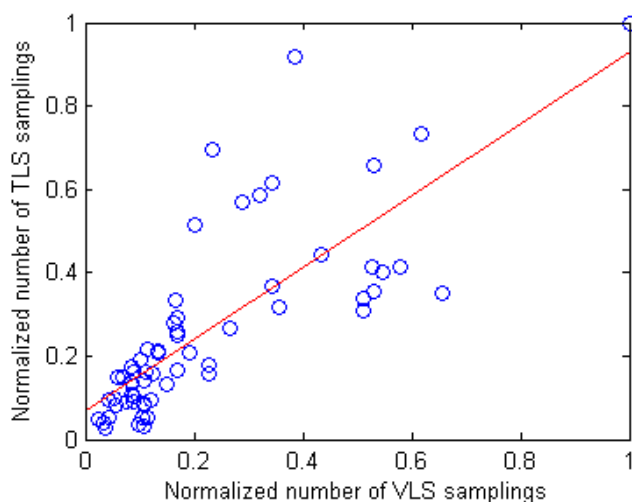


Table 1. The results of all the correlations after normalization. The slope and intercept relate to the lines-of-fit in Figures 5 and 6.

	R^2	RMSE	slope	intercept
TLS-Biomass _{Deciduous}	0.88	0.051	1.24	-0.088
TLS-Biomass _{Coniferous}	0.97	0.027	1.02	-0.031
VLS-TLS	0.61	0.076	0.86	0.069

5. Discussions and Conclusion

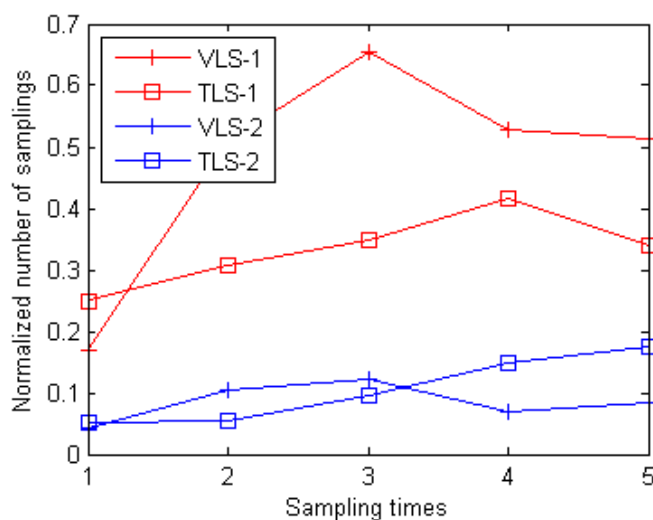
The linear relationship between VLS-samplings and biomass has been primarily verified. Based on the results yielded by this study, a VLS-based biomass investigation system can be established. The biomass of any tree within the scanning range of VLS can be retrieved, with the laboratory-tested results as linking references and the fitting function representing correlations as the bridging tool. This is greatly beneficial for biomass investigation in road environments. With the Sensei module system installed on airplanes, the proposed method can also be available for stand-wise and even region-wise forest. The distribution of forest biomass can be figured out explicitly, and then, can be applied as the fundamental geographic data by the strategy planners.

For the areas at the stand- and region-wise scales, number statistics of the samplings within crowns need instant segmentation of individual trees, and automatic methods are required to complete this task. Actually, the associated researches on automatic extraction of single trees from VLS point clouds have not been reported extensively [45]. In most cases, the VLS-associated segmentation still employs the approaches developed in ALS and TLS domains. Besides the advantage of quick sampling by VLS, the

proposed frame in this study can also use TLS as a space-expanding technique, which can supplement the areas investigation out of touch by VLS scanning, e.g., in road scenarios.

As the kernel variable, point number is subject to the density variations of foliages when growing, and different influences exist in VLS and TLS mapping. The inconsistent parts on crowns irradiated by VLS and TLS pulses worsen the interference. As shown in Figure 7, the impacts of the multi-factors can be reflected by the amplitude fluctuations of point numbers. The points sampled by VLS may decrease during foliages flourishing, while TLS-samplings increase for the same tree. At the same time, the extreme points of the trends from increasing to decreasing are not consistent for different trees. Therefore, seeking the appropriate foliages density in terms of the extreme point seems to be helpful for constructing more accurate retrieval models, but the complexity distribution and inclination of leaves makes this task extremely complicated. Obtaining the more accurate relationship of biomass and VLS samplings needs more works, and the synchronous images of crowns or intensity information of echoes may be fused into modeling for better performance.

Figure 7. Variations of the point numbers correspond to different measurement time and different trees, and the related performances are different for the VLS- and TLS-surveying modes. 1 and 2 refer to two trees. VLS-1 denotes the statistical results of the first crown investigated by VLS, and the other legends have the corresponding meanings.



The analysis of VLS and TLS scanning mechanisms discussed in sub-Section 3.3, actually aiming at the special apparatuses of Ibeo LUX and HDS6000, can be, indeed, generalized into a rule. This rule can be applicable for any other two kinds of laser scanning instruments. The factors can be deduced as follows: the arrangement of scan lines, the distance between scanners and objects, the angle between scan lines, the angle between the laser beams in each profile, the interval between parallel scan lines, the sampling frequency, the detecting capacity of multi-echoes per pulse, and *etc.* For other VLS and TLS systems, these factors can be checked to acquire the relationships of their samplings. Even for the same VLS systems, these factors sometimes must be considered to ensure the data is uniform under different situations, e.g., in stop-and-go mode or continuous-go mode.

As a conclusion, the applicability of VLS for biomass estimation at individual tree level is iterated, and this study fulfills the research gap of VLS-based biomass prediction. The theme of assessing the

ability of VLS for biomass retrieval through TLS samplings can make full usage of the previous work. VLS, TLS and destructive weighting here are combined to form a systematic methodology for accurate biomass surveying. With little trees measured by TLS in laboratory, the dilemma of felling big trees for artificial defoliation can be overcome, and the laborious relocations of TLS systems can be replaced by the stop-and-go mode of VLS. Biomass at individual tree level can be acquired efficiently with this advanced frame. If the system is further integrated with aerial platforms, the region-wise forests can be surveyed in an efficient way.

Acknowledgements

Thanks to the Academy of Finland for funding support through the following projects: Towards improved characterization of map objects, and Economy and technology of a global peer produced 3D geographical information system in the built environment. Thanks also to the Finnish Funding Agency for Technology and Innovation through the project: Development of automatic, detailed 3D model algorithms for forests and built environment.

References and Notes

1. Cihlar, J. Quantification of the regional carbon cycle of the biosphere: policy, science and land-use decisions. *J. Environ. Manag.* **2007**, *85*, 785-790.
2. Houghton, R.A. Aboveground forest biomass and the global carbon balance. *Glob. Chang. Biol.* **2005**, *11*, 945-958.
3. Houghton, R.A.; Hall, F.; Goetz, S.J. Importance of biomass in the global carbon cycle. *J. Geophys. Res.* **2009**, *114*, G00E03.
4. Hese, S.; Lucht, W.; Schimmlus, C.; Barnsley, M.; Dubayah, R.; Knorr, D.; Neumann, K.; Riedel, T.; Schröter, K. Global biomass mapping for an improved understanding of the CO₂ balance—The Earth observation mission carbon-3D. *Remote Sens. Environ.* **2005**, *94*, 94-104.
5. Holopainen, M.; Tuominen, S.; Karjalainen, M.; Hyypä, J.; Vastaranta, M.; Hyypä, H. The accuracy of high-resolution radar images in the estimation of plot-level forest variables. In *Advances in GIScience; Lecture Notes in Geoinformation and Cartography*; Springer: Berlin Heidelberg, Germany, 2009; pp. 67-82.
6. Anaya, J.A.; Chuvieco, E.; Palacios-Orueta, A. Aboveground biomass assessment in Colombia: A remote sensing approach. *Forest Ecol. Manag.* **2009**, *257*, 1237-1246.
7. Zheng, D.; Rademacher, J.; Chen, J.; Crow, T.; Bresee, M.; Le Moine, J.; Ryu, S.R. Estimating aboveground biomass using Landsat 7 ETM + data across a managed landscape in northern Wisconsin, USA. *Remote Sens. Environ.* **2004**, *93*, 402-411.
8. Wessels, K.J.; Prince, S.D.; Zambatis, N.; Macfadyen, S.; Frost, P.E.; Van Zyl, D. Relationship between herbaceous biomass and 1-km² advanced very high resolution radiometer (AVHRR) NDVI in Kruger National Park, South Africa. *Int. J. Remote Sens.* **2006**, *27*, 951-973.
9. Suganuma, H.; Abe, Y.; Taniguchi, M.; Tanouchi, H.; Utsugi, H.; Kojima, T.; Yamada, K. Stand biomass estimation method by canopy coverage for application to remote sensing in an arid area of Western Australia. *Forest Ecol. Manag.* **2006**, *222*, 75-87.

10. Hansen, M.C.; DeFries, R.S.; Townsend, J.R.G.; Carroll, M.; Dimiceli, C.; Sohlberg, R. Global percent tree cover at a spatial resolution of 500 meters: First results of the MODIS vegetation continuous algorithm. *Earth Interactions* **2003**, *7*, 1-15.
11. Lefsky, M.A.; Cohen, W.B.; Parker, G.G.; Harding, D.J. LiDAR remote sensing for ecosystem studies. *Bioscience* **2002**, *52*, 19-30.
12. Holopainen, M.; Haapanen, R.; Karjalainen, M.; Vastaranta, M.; Hyyppä, J.; Yu, X.; Tuominen, S.; Hyyppä, H. Combination of low-pulse ALS data and TerraSAR-X radar images in the estimation of plot-level forest variables. In *Proceedings of Laserscanning09*, Paris, France, 2009; In *The International Archives of the Photogrammetry, Remote Sensing and Spatial Information Sciences*; ISPRS: Vienna, Austria, 2009; Volume 38, Part 3/W8, pp. 135-140.
13. Næsset, E. Predicting forest stand characteristics with airborne scanning laser using a practical two-stage procedure and field data. *Remote Sens. Environ.* **2002**, *80*, 88-99.
14. Hyyppä, J.; Inkinen, M. Detecting and estimating attributes for single trees using laser scanner. *The Photogramm. J. Fin.* **1999**, *16*, 27-42.
15. Solberg, S.; Næsset, E.; Hanssen, K.H.; Christiansen, E. Mapping defoliation during a severe insect attack on Scots pine using airborne laser scanning. *Remote Sens. Environ.* **2006**, *102*, 364-376.
16. Zhao, K.; Popescu, S.; Nelson, R. Lidar remote sensing of forest biomass: A scale-invariant estimation approach using airborne lasers. *Remote Sens. Environ.* **2009**, *113*, 182-196.
17. Hawbaker, T.J.; Keuler, N.S.; Lesak, A.A.; Gobakken, T.; Contrucci, K.; Radeloff, V.C. Improved estimates of forest vegetation structure and biomass with a LiDAR-optimized sampling design. *J. Geophys. Res.* **2009**, *114*, G00E04.
18. St-Onge, B.; Hu, Y.; Vega, C. Mapping the height and above-ground biomass of a mixed forest using lidar and stereo Ikonos images. *Int. J. Remote Sens.* **2008**, *29*, 1277-1294.
19. Lucas, R.M.; Lee, A.C.; Bunting, P.J. Retrieving forest biomass through integration of CASI and LiDAR data. *Int. J. Remote Sens.* **2008**, *29*, 1553-1577.
20. Popescu, S.C.; Wynne, R.H.; Nelson, R.H. Estimating plot-level tree heights with LIDAR: Local filtering with a canopy-height based variable window size. *Comput. Electron. Agr.* **2002**, *37*, 71-95.
21. Chen, Q.; Baldocchi, D.; Gong, P.; Kelly, M. Isolating individual trees in a Savanna woodland using small footprint lidar data. *Photogramm. Eng. Remote Sensing* **2006**, *72*, 923-932.
22. Næsset, E. Practical large-scale forest stand inventory using a small footprint airborne scanning laser. *Scand. J. Forest Res.* **2004**, *19*, 164-179.
23. Andersen, H.E.; McGaughey, R.J.; Reutebuch, S.E. Estimating forest canopy fuel parameters using lidar data. *Remote Sens. Environ.* **2005**, *94*, 441-449.
24. Mutlu, M.; Popescu, S.C.; Stripling, C.; Spencer, T. Assessing surface fuel models using lidar and multispectral data fusion. *Remote Sens. Environ.* **2008**, *112*, 274-285.
25. Popescu, S.C. Estimating biomass of individual pine trees using airborne lidar. *Biomass Bioenerg.* **2007**, *31*, 646-655.
26. Hosoi, F.; Omasa, K. Voxel-based 3-D modeling of individual trees for estimating leaf area density using high-resolution portable scanning Lidar. *IEEE Trans. Geosci. Remote Sens.* **2006**, *44*, 3610-3618.

27. Kaasalainen, S.; Krooks, A.; Kukko, A.; Kaartinen, H. Radiometric calibration of terrestrial laser scanners with external reference targets. *Remote Sens.* **2009**, *1*, 144-158.
28. Lovell, J.L.; Jupp, D.L.B.; Culvenor, D.S.; Coops, N.C. Using airborne and ground-based ranging lidar to measure canopy structure in Australian forests. *Can. J. Remote Sens.* **2003**, *29*, 607-622.
29. Jupp, D.L.B.; Culvenor, D.S.; Lovell, J.L.; Newnham, G.J.; Strahler, A.H.; Woodcock, C.E. Estimating forest LAI profiles and structural parameters using a ground based laser called "Echidna". *Tree Physiol.* **2008**, *29*, 171-181.
30. Radtke, P.J.; Bolstad, P.V. Laser point-quadrat sampling for estimating foliage-height profiles in broad-leaved forests. *Can. J. Forest Res.* **2001**, *31*, 410-418.
31. Maltamo, M.; Eerikäinen, K.; Pitkänen, J.; Hyyppä, J.; Vehmas, M. Estimation of timber volume and stem density based on scanning laser altimetry and expected tree size distribution functions. *Remote Sens. Environ.* **2004**, *90*, 319-330.
32. Omasa, K.; Urano, Y.; Oguma, H.; Fujinuma, Y. Mapping of tree position of *Larix leptolepis* woods and estimation of diameter at breast height (DBH) and biomass of the trees using range data measured by a portable scanning lidar. *J. Remote Sens. Soc. Jpn.* **2002**, *22*, 550-557.
33. Hunter, G.; Cox, C.; Kremer, J. Development of a Commercial laser scanning mobile mapping system-StreetMapper. In *Proceedings of Second International Workshop on the Future of Remote Sensing*, Antwerp, Belgium, October 2006.
34. Kukko, A.; Andrei, C.O.; Salminen, V.M.; Kaartinen, H.; Chen, Y.; Rönholm, P.; Hyyppä, H.; Hyyppä, J.; Chen, R.; Haggren, H.; Kosonen, I.; Capek, K. Road environment mapping system of the Finnish Geodetic Institute-FGI ROAMER. In *Proceedings of the ISPRS Workshop 'Laser Scanning 2007 and SilviLaser 2007'*, Espoo, Finland, 2007; In *The International Archives of the Photogrammetry, Remote Sensing and Spatial Information Sciences*; ISPRS: Vienna, Austria, 2007; Volume XXXVI, Part 3/W52, pp. 241-247.
35. Zampa, F.; Conforti, D. Mapping with mobile Lidar. *GIM Int.* **2009**, *23*, 35-37.
36. Ussyshkin, V. Mobile laser scanning technology for surveying applications: From data collection to end-products. In *FIG Working Week 2009: Surveyors Key Role in Accelerated Development*, Eilat, Israel, May 2009.
37. Tao, C.V. Mobile mapping technology for road network data acquisition. *J. Geospatial Eng.* **2000**, *2*, 1-13.
38. Zhao, H.; Shibasaki, R. A vehicle-borne urban 3-D acquisition system using single-row laser range scanners. *IEEE Trans. Syst. Man Cybern. B* **2003**, *33*, 658-666.
39. Früh, C.; Jain, S.; Zakhor, A. Data processing algorithms for generating textured 3D building façade meshes from laser scans and camera images. *Int. J. Comput. Vis.* **2005**, *61*, 159-184.
40. Goulette, F.; Nashashibi, F.; Abuhadrous, I.; Ammoun, S.; Lurgeau, C. An integrated on-board laser range sensing system for on-the-way city and road modelling. In *Proceedings of the ISPRS Commission I Symposium "From Sensors to Imagery"*, Paris, France, July 2006.
41. Yu, S.J.; Sukumar, S.R.; Koschan, A.F.; Page, D.L.; Abidi, M.A. 3D reconstruction of road surfaces using an integrated multi-sensory approach. *Opt. Lasers Eng.* **2007**, *45*, 808-818.
42. Jaakkola, A.; Hyyppä, J.; Hyyppä, H.; Kukko, A. Retrieval algorithms for road surface modelling using Laser-based mobile mapping. *Sensors* **2008**, *8*, 5238-5249.

43. Hernandez, J.; Marcotegui, B. Filtering of artifacts and pavement segmentation from mobile lidar data. In *Laser scanning 2009 IAPRS*, Paris, France, September 2009; In *The International Archives of the Photogrammetry, Remote Sensing and Spatial Information Sciences*; ISPRS: Vienna, Austria, 2009; Volume XXXVIII, Part 3/W8, pp. 329-333.
44. Anon. *TerraScan User's Guide*; Terrasolid, Helsinki, Finland, 2004. Available online: <http://terrasolid.fi> (accessed on 28 June 2010).
45. Lin, Y.; Hyypä, J.; Jaakkola, A.; Yu, X. Three-level frame and RD-schematic algorithm for automatic recognition of individual trees from VLS point clouds. *Int. J. Remote Sens.* **2010**, Submitted.

© 2010 by the authors; licensee MDPI, Basel, Switzerland. This article is an Open Access article distributed under the terms and conditions of the Creative Commons Attribution license (<http://creativecommons.org/licenses/by/3.0/>).